Supplementary Material for

Extension and application of an observation-based local climate index aimed to anticipate the impact of ENSO events on Colombia

Juan-Manuel Sayol[1], Laura M. Vásquez[2], Jorge L. Valencia[2], Jean R. Linero-Cueto[3],

David García-García[1], Isabel Vigo[1], Alejandro Orfila[4]

[1]Department of Applied Mathematics, University of Alicante, 03690 Sant Vicent del Raspeig, Alicante, Spain

[2]Dirección General Marítima, Centro de Investigaciones Oceanográficas e Hidrográficas del Pacífico, (Dimar-CCCP). Vía El Morro, Capitanía de Puerto, Tumaco, Nariño, Colombia

[3]Facultad de Ingeniería, Universidad del Magdalena, Carrera 32 # 22-08, Santa Marta, Colombia

[4]Instituto Mediterráneo de Estudios Avanzados (CSIC-UIB), 07190 Esporles, Balearic Islands, Spain

Contents:

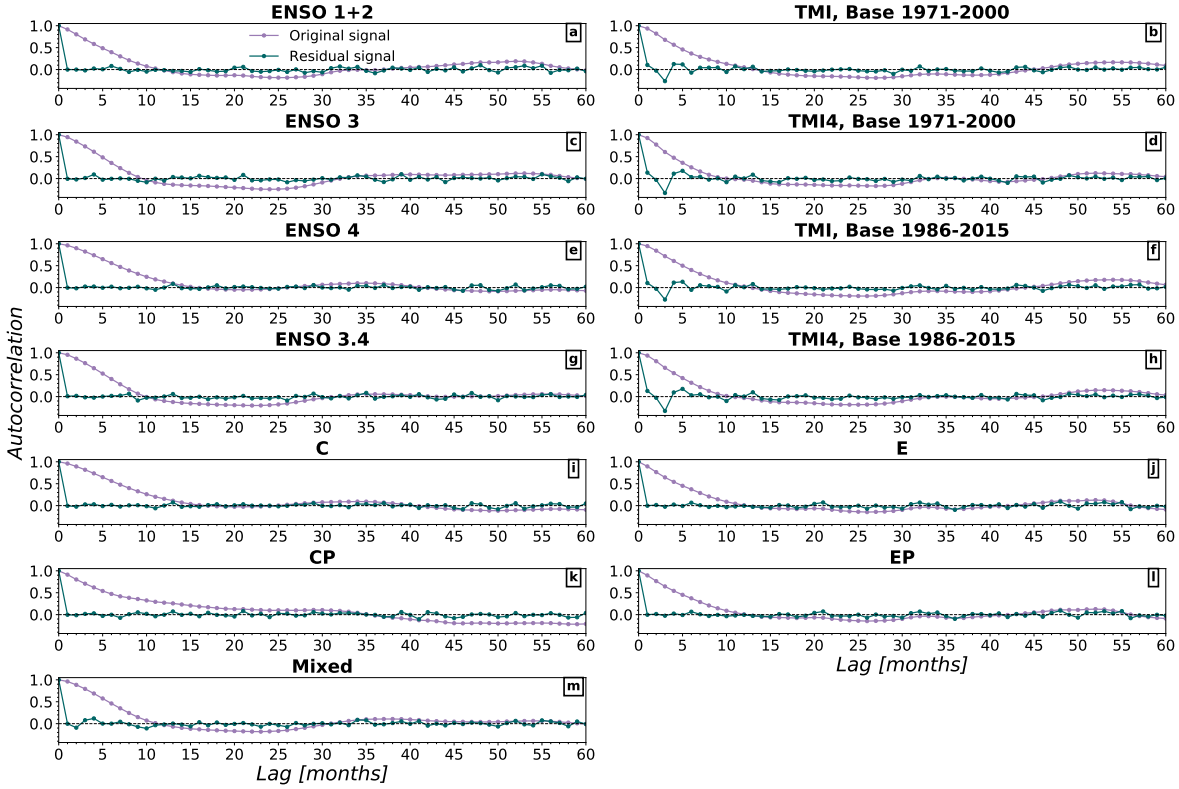

FIGURE S1 Autocorrelation of original signals and residual components of ENSO NOAA oceanic indexes (a)-(c)-(e)-(g), of TMI study cases shown in Fig. 4 (b)-(d)-(f)-(h) and of ENSO indexes derived by Takahashi et al. (2011) (i)-(j), and Sullivan et al. (2016) (k)-(l)-(m). Residual components are computed by applying a SARIMA model in which seven parameters (p,d,q)(P,D,Q)m are adjusted: p is the trend autoregression order, d the trend difference order, q the trend moving average order, P the seasonal autoregressive order, D the seasonal difference order, Q the seasonal moving average order and m the number of time steps for a single seasonal period (e.g. 12 months for Earth's seasonality). Unit of time lag is month.

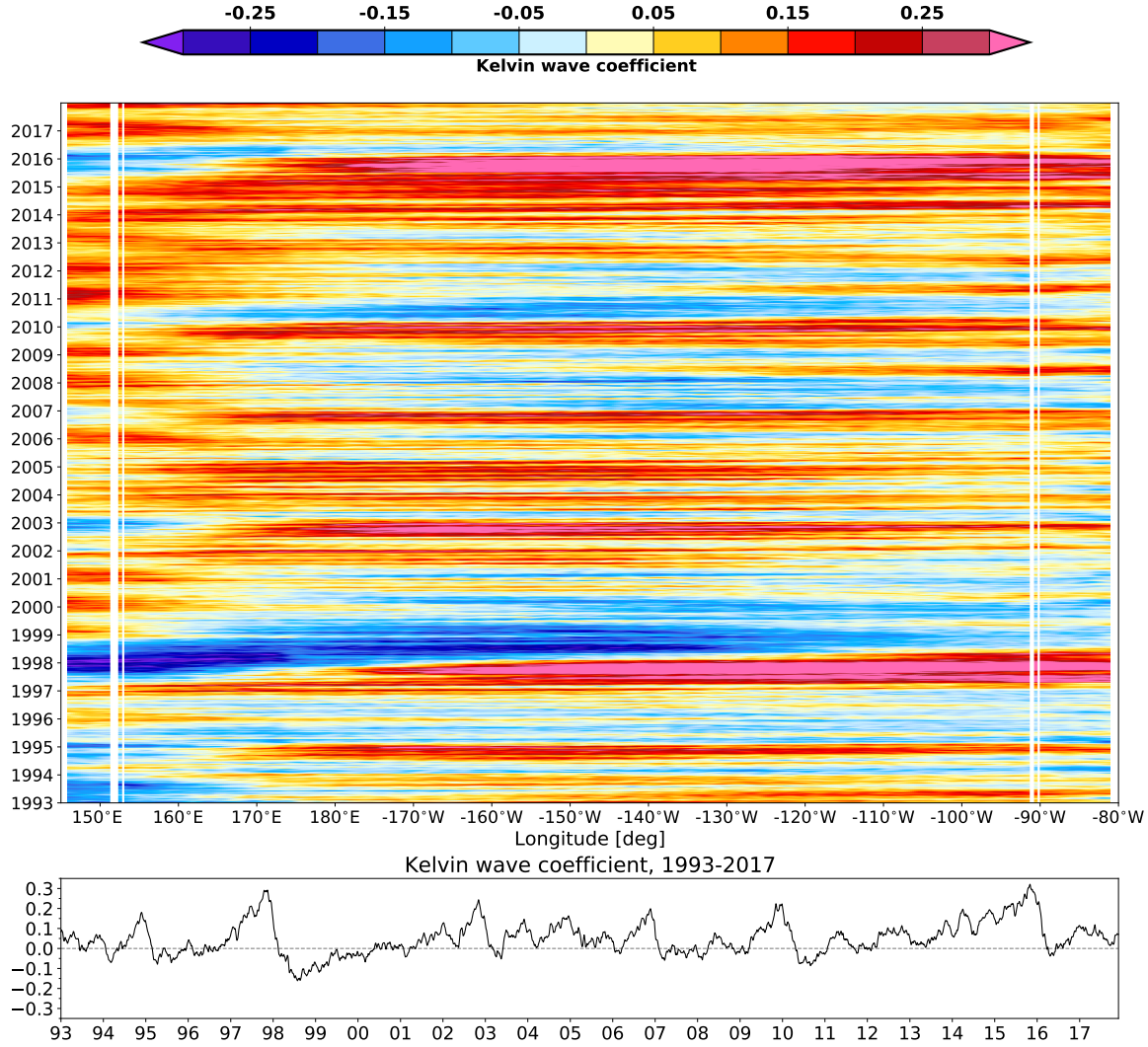

FIGURE S2 (top panel) Hovmöller diagram depicting the zonal propagation of Kelvin waves along the equatorial Pacific Ocean between years 1993 and 2017 (both included). (bottom panel) Time series of the zonally-averaged Kelvin sea level anomalies over the equatorial Pacific Ocean (between 145°E and the Pacific coast of Colombia between -4°S and 4°N of latitude). Note that the strongest positive anomalies are found for El Niño 1997/1998 and El Niño 2015/2016. Vertical white lines are due to a noisy effect of islands.

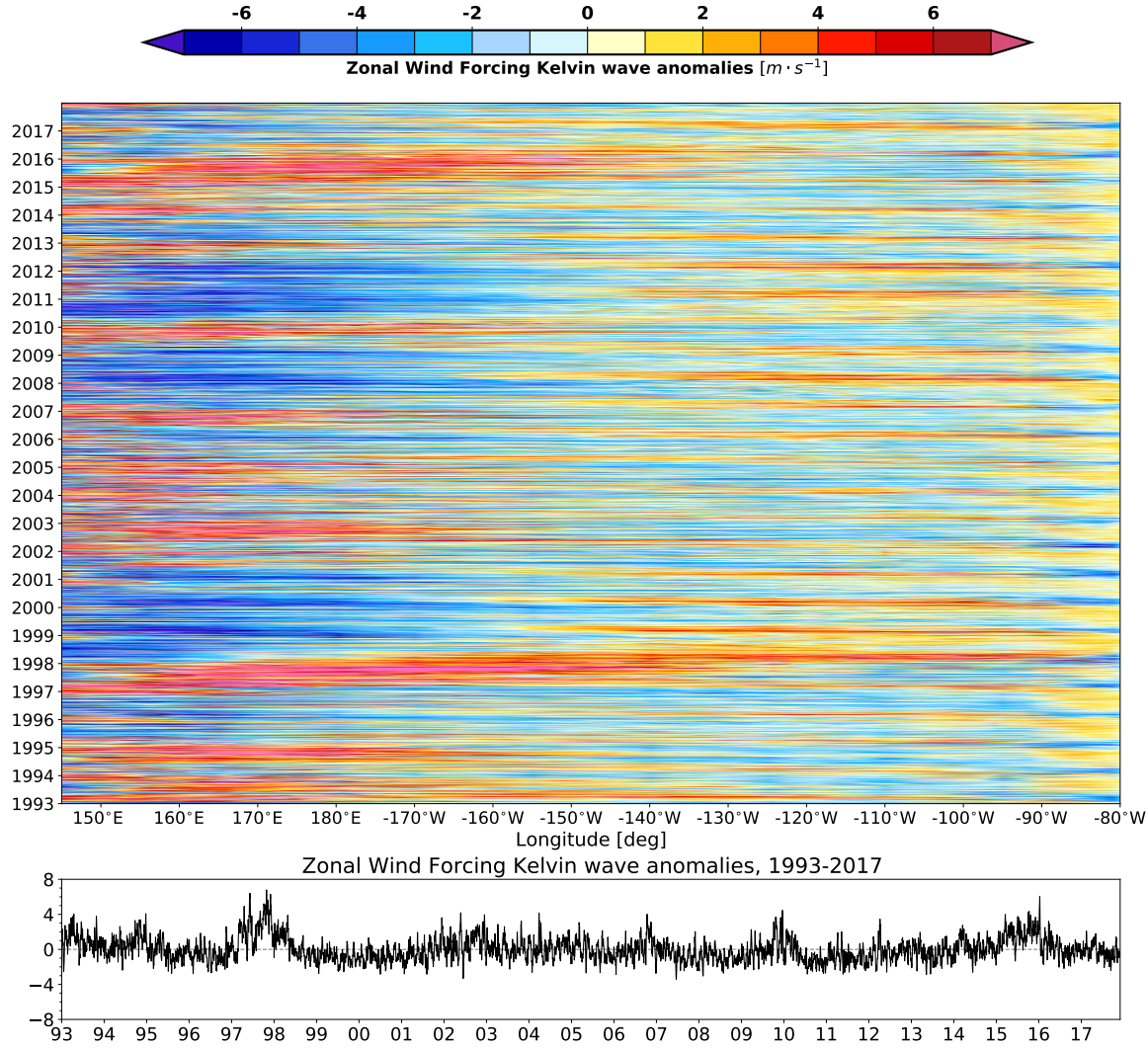

FIGURE S3 (top panel) Hovmöller diagram illustrating the zonal propagation of wind-forcing associated to Kelvin waves along equatorial Pacific Ocean between years 1993 and 2017 (both included). (bottom panel) Time series of zonally-averaged Kelvin sea level anomalies over the equatorial Pacific Ocean (between 145°E and the Pacific coast of Colombia between -4°S and 4°N of latitude). Note that the strongest positive anomalies are found for El Niño 1997/1998 and El Niño 2015/2016.

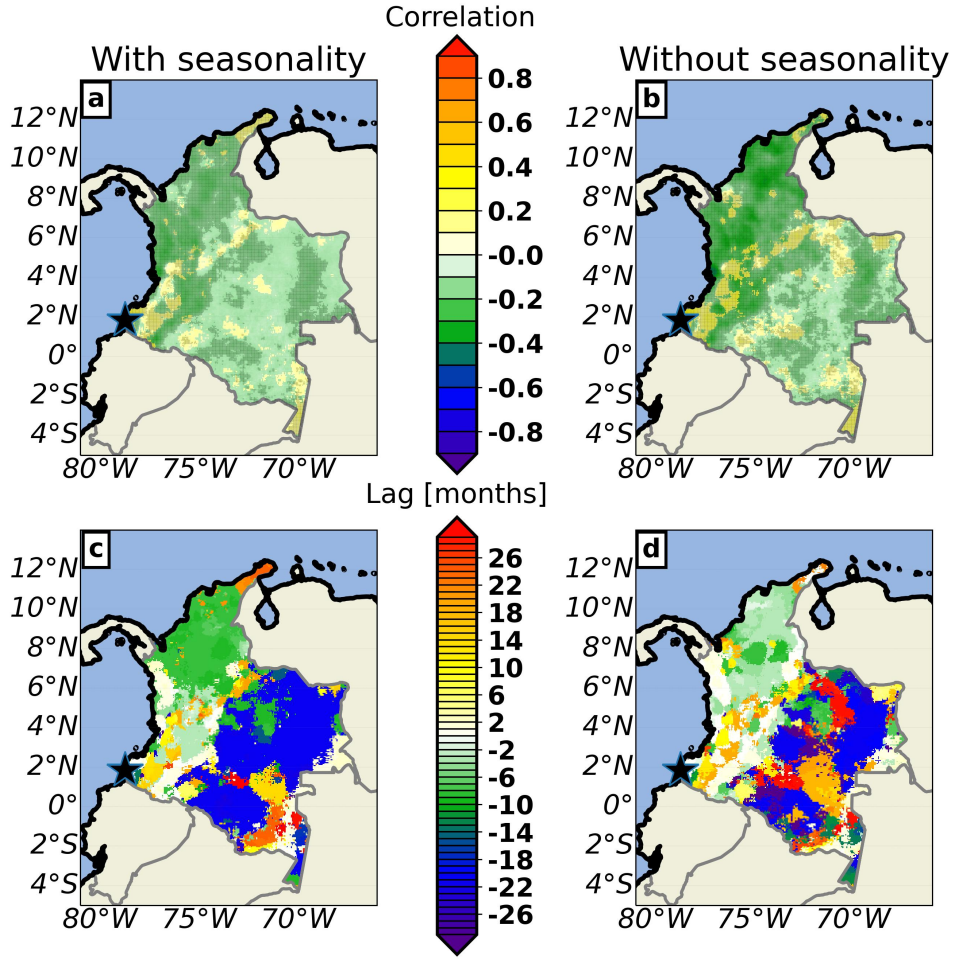

FIGURE S4 (a)-(c) Maps of cross-correlation between the TMI and the time series of CHIRPS rain associated with every grid cell between years 1983 and 2017. The largest correlation (in absolute value) is shown with shading for two cases: (a) with seasonal cycle and (c) without the seasonal cycle. The seasonal cycle has been removed by subtracting the corresponding monthly climatology (1983–2017) to each time series. Hash lines indicate that correlations are significant at 99% according to a t-Student two-tailed distribution. Maps of time lag for the above correlation maps are shown in bottom panels for rain data including (b) and not including (d) the seasonal cycle. Negative (positive) time lags mean that the TMI varies some time earlier (later) than rain (the number of months is indicated in the colorbar). The white color indicates that variations are nearly simultaneous.

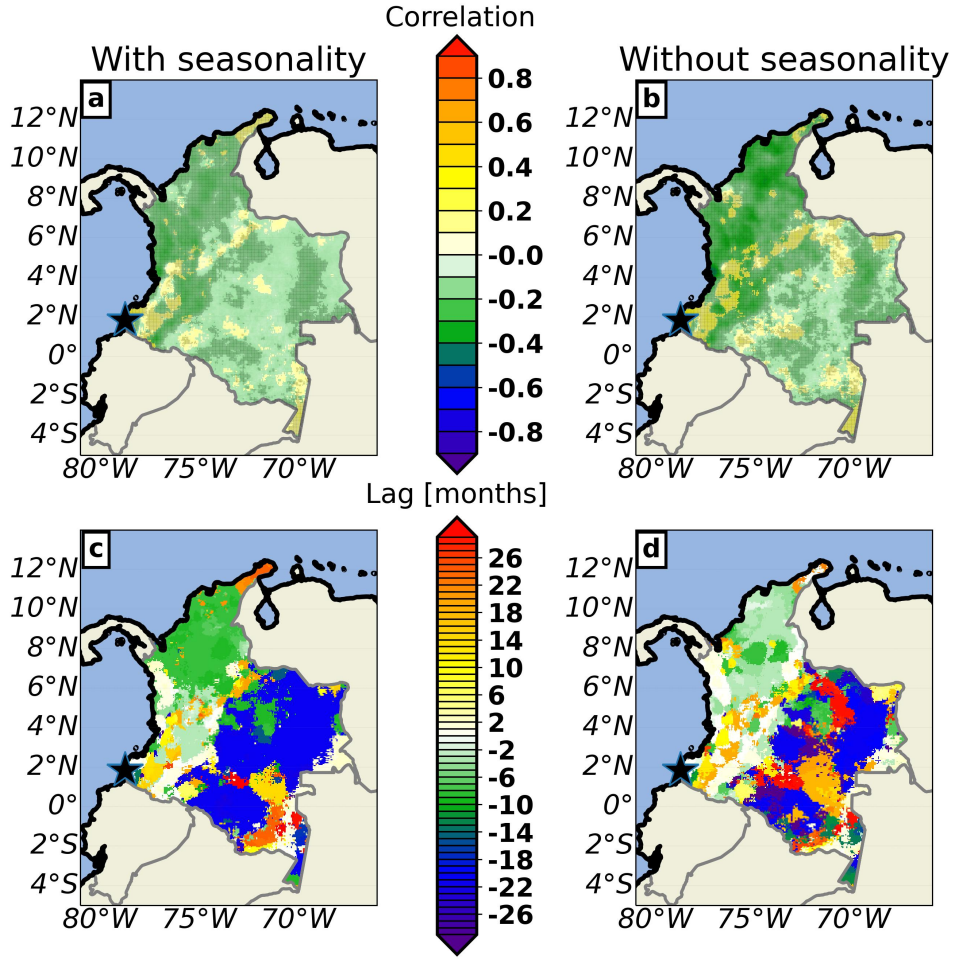

FIGURE S5 (a)-(c) Maps of cross-correlation between the ENSO 1+2 and the time series of CHIRPS rain associated with every grid cell between years 1983 and 2017. The largest correlation (in absolute value) is shown with shading for two cases: (a) with seasonal cycle and (c) without the seasonal cycle. The seasonal cycle has been removed by subtracting the corresponding climate monthly mean (1983-2017) to each time series. Hash lines indicate that correlations are significant at 99% according to a t-Student two-tailed distribution. Maps of time lag for the above correlation maps are shown in bottom panels for rain data including (b) and not including (d) the seasonal cycle. Negative (positive) time lags mean that the ENSO 1+2 varies some time earlier (later) than rain (the number of months is indicated in the colorbar). The white color indicates that variations are nearly simultaneous.

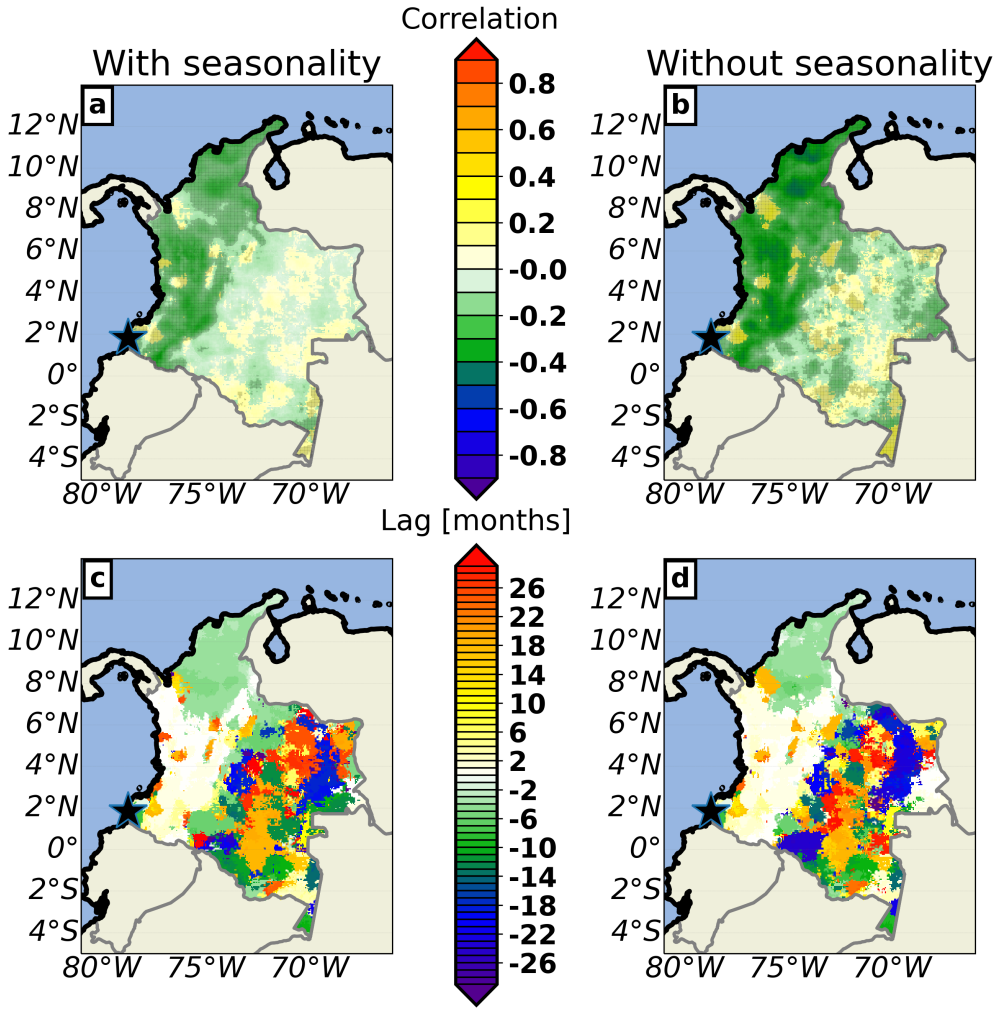

FIGURE S6 (a)-(c) Maps of cross-correlation between the ENSO 3 and the time series of CHIRPS rain associated with every grid cell between years 1983 and 2017. The largest correlation (in absolute value) is shown with shading for two cases: (a) with seasonal cycle and (c) without the seasonal cycle. The seasonal cycle has been removed by subtracting the corresponding monthly climatology (1983-2017) to each time series. Hash lines indicate that correlations are significant at 99% according to a t-Student two-tailed distribution. Maps of time lag for the above correlation maps are shown in bottom panels for rain data including (b) and not including (d) the seasonal cycle. Negative (positive) time lags mean that the ENSO 3 varies some time earlier (later) than rain (the number of months is indicated in the colorbar). The white color indicates that variations are nearly simultaneous.

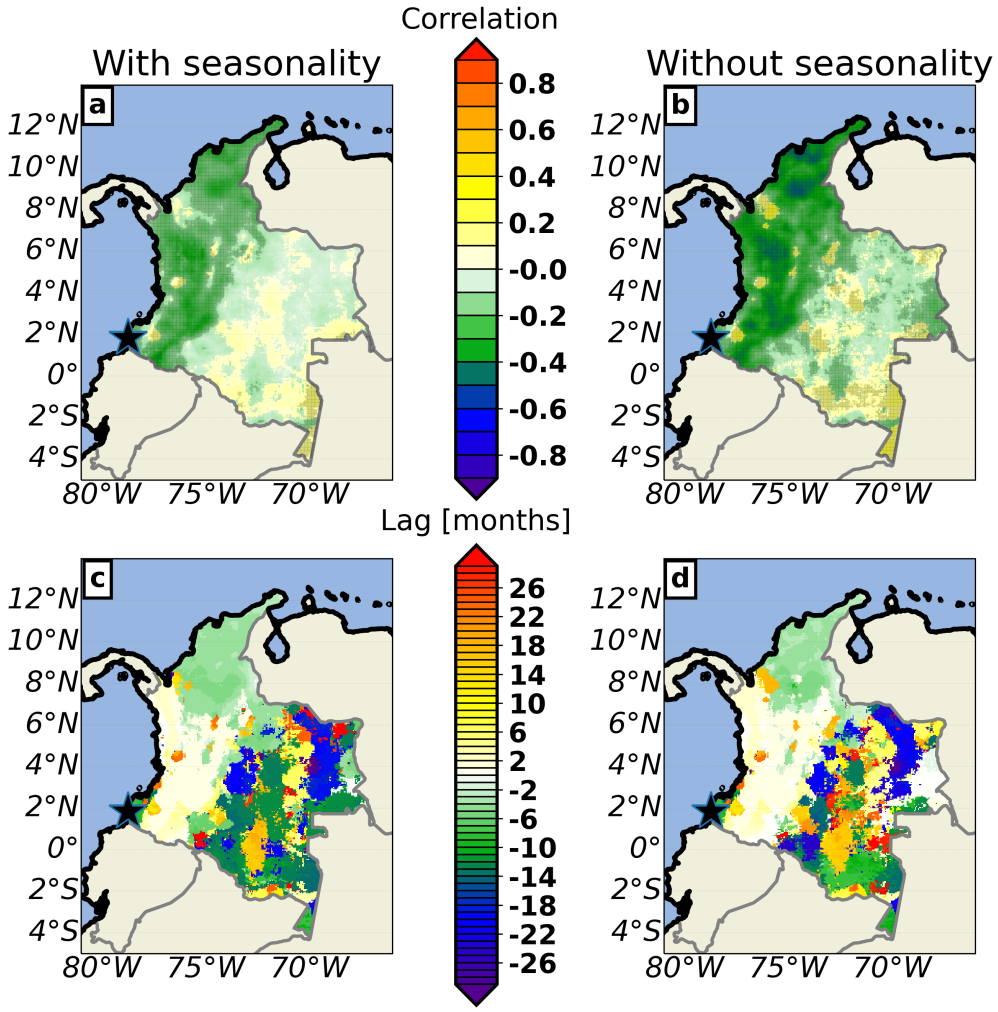

FIGURE S7 (a)-(c) Maps of cross-correlation between the ENSO 3.4 and the time series of CHIRPS rain associated with every grid cell between years 1983 and 2017. The largest correlation (in absolute value) is shown with shading for two cases: (a) with seasonal cycle and (c) without the seasonal cycle. The seasonal cycle has been removed by subtracting the corresponding monthly climatology (1983-2017) to each time series. Hash lines indicate that correlations are significant at 99% according to a t-Student two-tailed distribution. Maps of time lag for the above correlation maps are shown in bottom panels for rain data including (b) and not including (d) the seasonal cycle. Negative (positive) time lags mean that the ENSO 3.4 varies some time earlier (later) than rain (the number of months is indicated in the colorbar). The white color indicates that variations are nearly simultaneous.

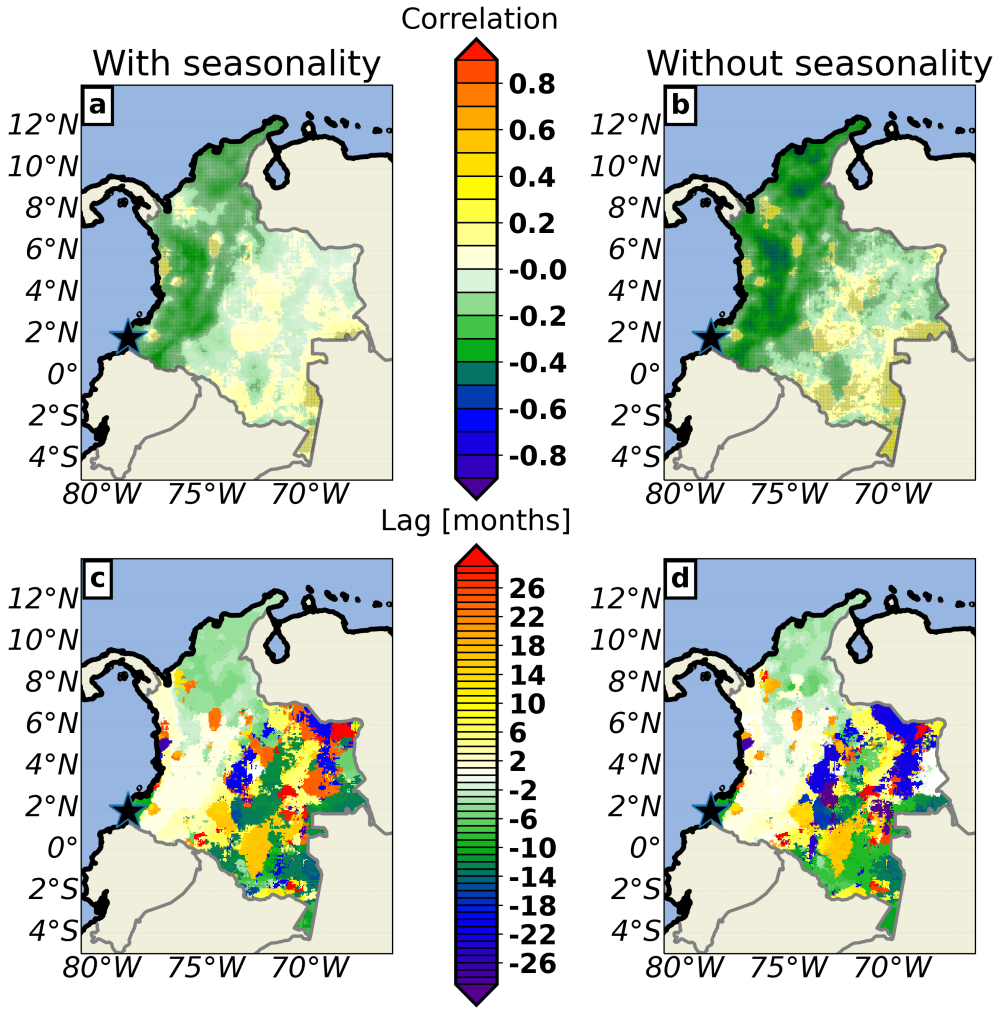

FIGURE S8 (a)-(c) Maps of cross-correlation between the ENSO 4 and the time series of CHIRPS rain associated with every grid cell between years 1983 and 2017. The largest correlation (in absolute value) is shown with shading for two cases: (a) with seasonal cycle and (c) without the seasonal cycle. The seasonal cycle has been removed by subtracting the corresponding monthly climatology (1983-2017) to each time series. Hash lines indicate that correlations are significant at 99% according to a t-Student two-tailed distribution. Maps of time lag for the above correlation maps are shown in bottom panels for rain data including (b) and not including (d) the seasonal cycle. Negative (positive) time lags mean that the ENSO 4 varies some time earlier (later) than rain (the number of months is indicated in the colorbar). The white color indicates that variations are nearly simultaneous.

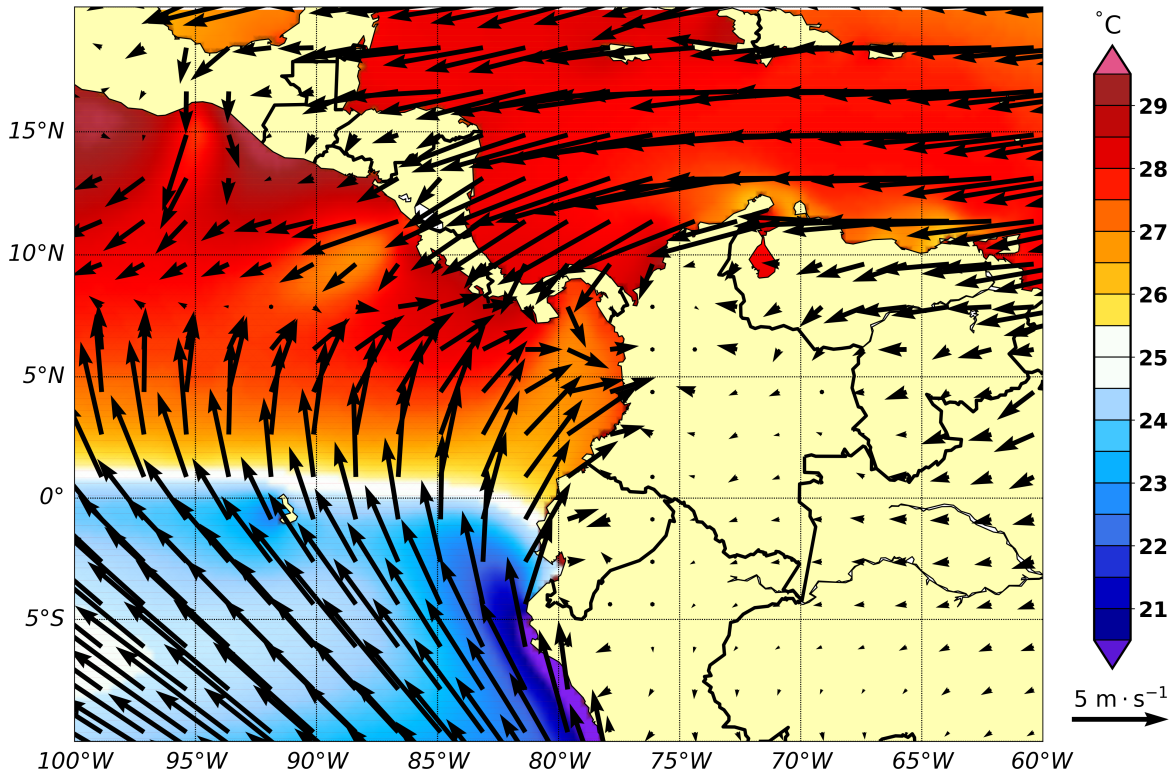

FIGURE S9 Map showing the mean SST field (shading), and mean surface wind (black arrows) during years 1988–2017. Data is described in section 3. For the sake of clarity, only 1 of every 7 arrows are shown.

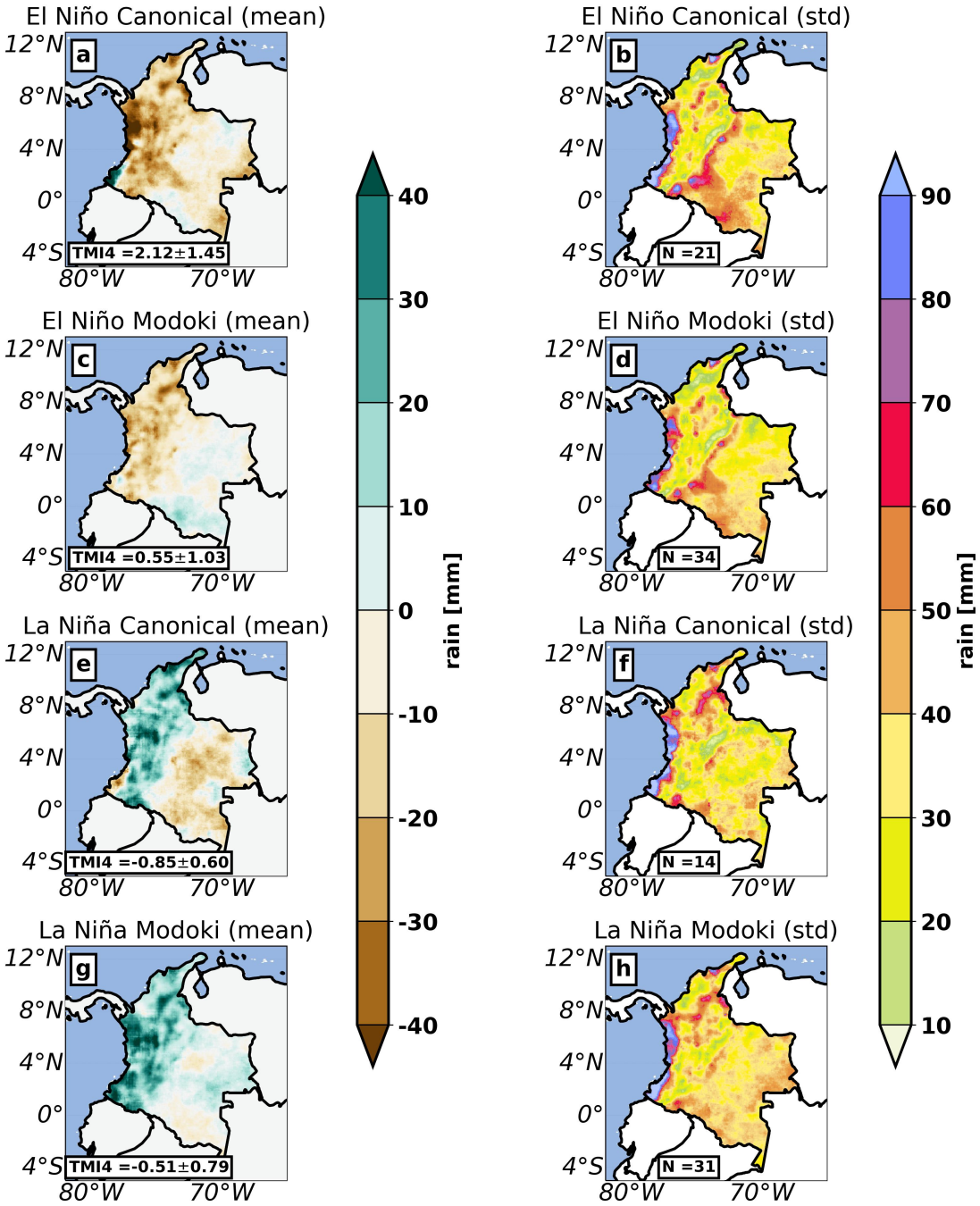

FIGURE S10 Mean (panels a-c-e-g) and standard deviation (panels b-d-f-h) composites of rainfall anomalies for different ENSO types. The selected months associated to main ENSO types are retrieved from Table 2 of Navarro-Monterroza et al. (2019) and these months are indicated in Fig. 13. Note that rainfall anomalies are computed by subtracting the monthly climatology at each grid cell. The climatology covers the period 1983–2017. Note that N (included inside the standard deviation panels of right panels) refers to the number of trimesters used to perform each composite (i.e. the number of total monthly maps is N×3.)

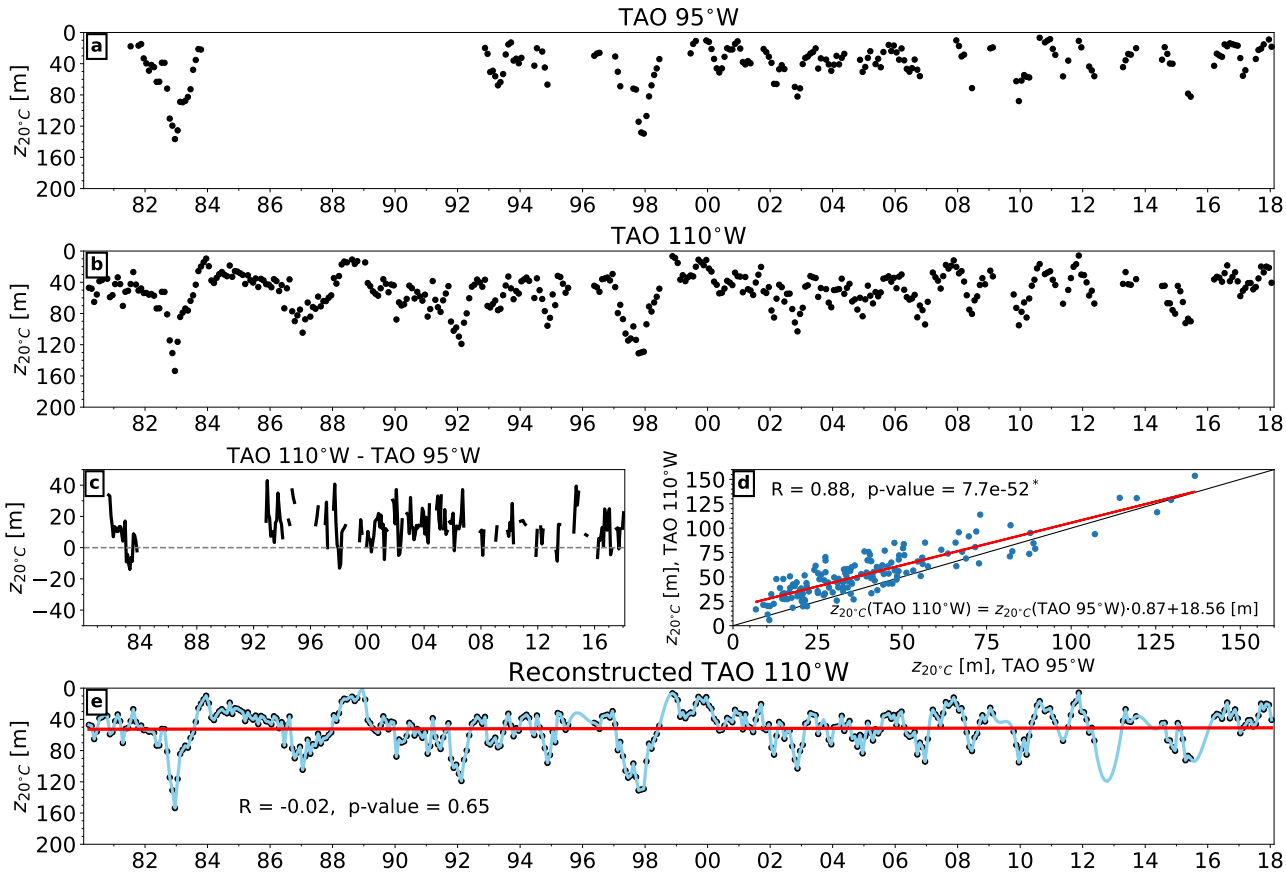

FIGURE S11 (a) Time series of 20°C isotherm depth ($z_{20°C}$) at 95°W from Tropical Atmosphere Ocean project (TAO) data; (b) Time series of $z_{20°C}$ at 110°W from TAO; (c) Time series of the difference between $z_{20°C}$ at 110°W and at 95°W; (d) Scatter diagram between $z_{20°C}$ at 95°W and at 110°W, where the red line represents a linear fit between both depths; (e) original time series of $z_{20°C}$ at 110°W (black points) and the reconstructed time series OF $z_{20°C}$ at 110°W (sky blue solid line) after filling gaps with 95°W data and performing a quadratic interpolation. TAO data was downloaded from: `https://www.pmel.noaa.gov/gtmba/pmel-theme/pacific-ocean-tao`.

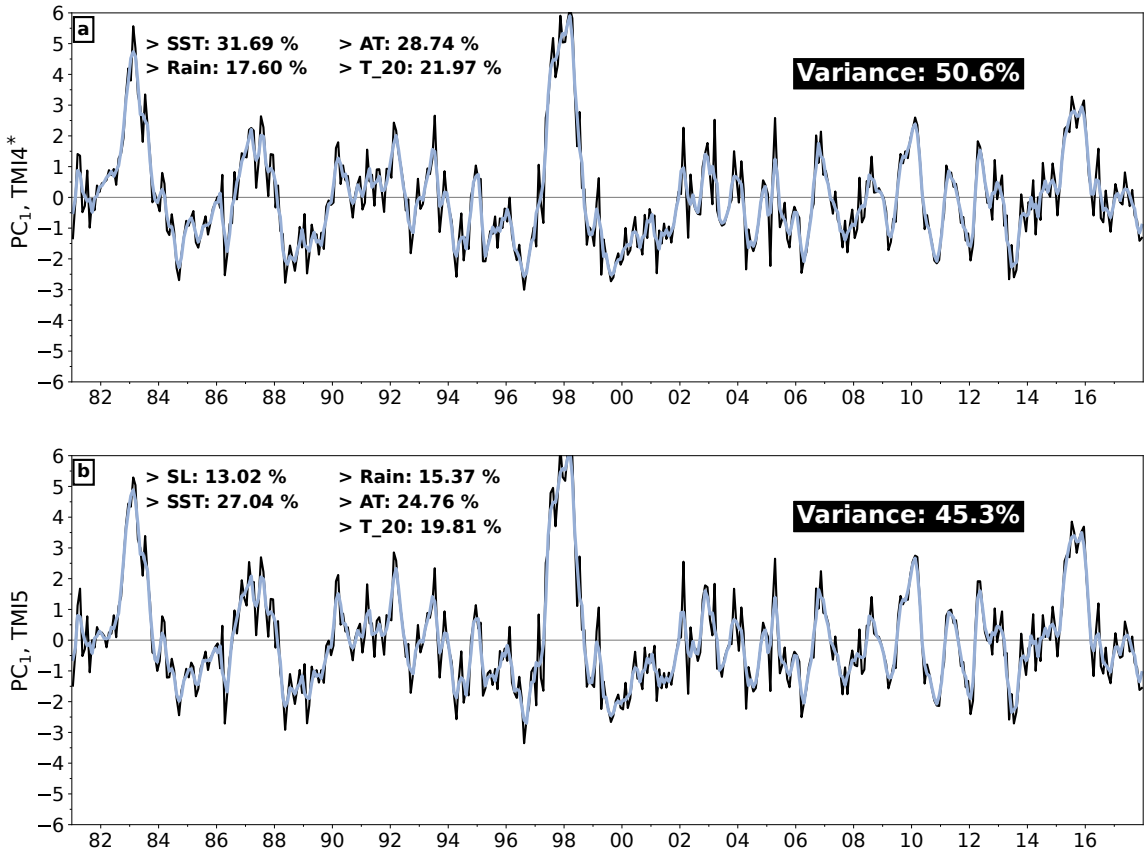

FIGURE S12 Time series of TMI4* (a, 20°C isotherm depth instead of sea level), and TMI5 (b, 20°C isotherm depth is added to the original TMI4. TMI4* and TMI5 are shown for the base period 1986–2015, since $z_{20°C}$ is only available from 1981. The black line denotes the first component (the one that explains most variance, PC_1) obtained from the PCA analysis (section 3.7 of the Manuscript). The gray line is the 3-month average of PC_1, which is as the indexes are defined (Rodríguez-Rubio, 2013). Variables used in each case and their weight in the construction of modified TMI4 and TMI5, as well as the explained variance by the PC_1 are shown in the top-left and in the top-right of each panel, respectively.

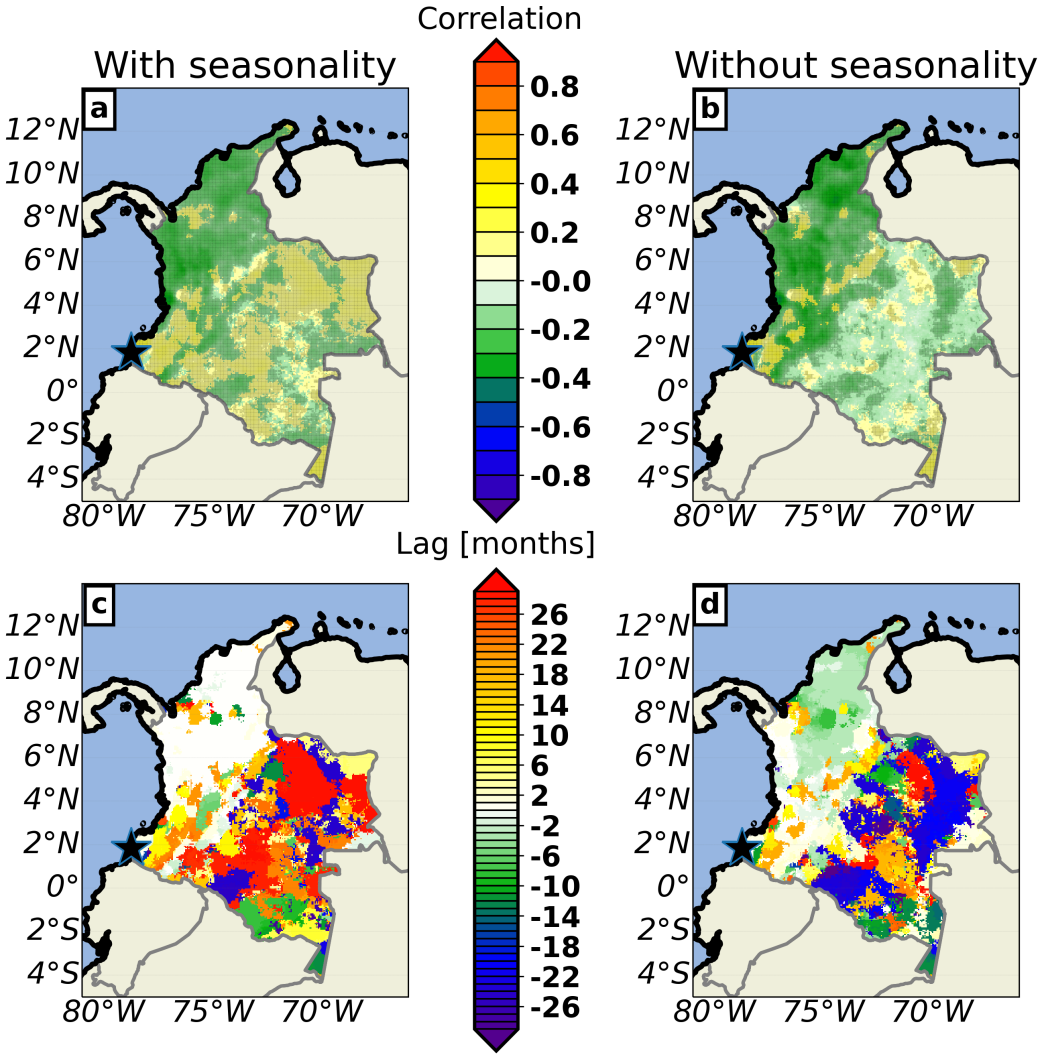

FIGURE S13 (a)-(b) Maps of cross-correlation between TMI4* (which includes the 20°C isotherm depth instead of sea level) and the time series of CHIRPS rain associated with every grid cell between years 1983 and 2017. The largest correlation (in absolute value) is shown with shading for two cases: (a) with seasonal cycle and (c) without the seasonal cycle. The seasonal cycle has been removed by subtracting the corresponding monthly climatology (1983–2017) to each timeseries. Hash lines indicate that correlations are significant at 99% according to a t-Student two-tailed distribution. Maps of time lag for the above correlation maps are shown in bottom panels for rain data including (c) and not including (d) the seasonal cycle. Negative (positive)time lags mean that TMI4 varies some time earlier (later) than rain (the number of months is indicated in the colorbar). The white color indicates that variations are nearly simultaneous.

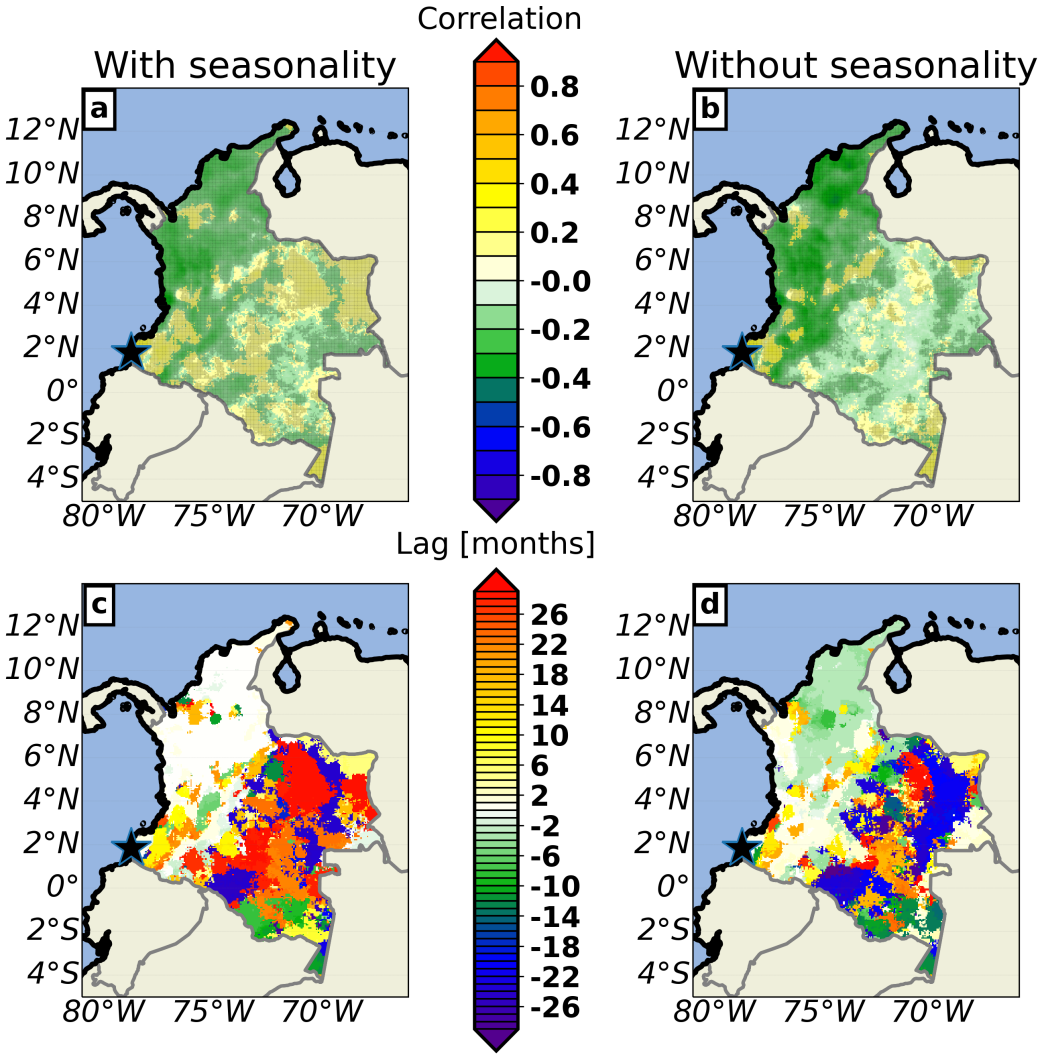

FIGURE S14 (a)-(b) Maps of cross-correlation between TMI5 and the time series of CHIRPS rain associated with every grid cell between years 1983 and 2017. The largest correlation (in absolute value) is shown with shading for two cases: (a) with seasonal cycle and (c) without the seasonal cycle. The seasonal cycle has been removed by subtracting the corresponding monthly climatology (1983–2017) to each timeseries. Hash lines indicate that correlations are significant at 99% according to a t-Student two-tailed distribution. Maps of time lag for the above correlation maps are shown in bottom panels for rain data including (c) and not including (d) the seasonal cycle. Negative (positive)time lags mean that TMI4 varies some time earlier (later) than rain (the number of months is indicated in the colorbar). The white color indicates that variations are nearly simultaneous.

Department	Rainfall: $\overline{x} \pm \sigma$ [mm]
Amazonas	3418 ± 294
Antioquia	3073 ± 329
Arauca	2135 ± 245
Atlántico	1032 ± 247
Bolívar	2192 ± 319
Boyacá	1738 ± 220
Córdoba	2218 ± 217
Caldas	2618 ± 346
Caquetá	3179 ± 296
Casanare	2290 ± 249
Cauca	3229 ± 426
Cesar	1662 ± 292
Chocó	5420 ± 601
Cundinamarca	1691 ± 209
Guainía	3299 ± 288
Guaviare	3113 ± 273
Huila	1624 ± 239
La Guajira	874 ± 240
Magdalena	1537 ± 287
Meta	2736 ± 266
Nariño	3079 ± 498
Norte de Santander	2102 ± 329
Putumayo	3389 ± 366
Quindío	2004 ± 243
Risaralda	2749 ± 310
Santander	2338 ± 257
Sucre	1737 ± 275
Tolima	1823 ± 281
Valle del Cauca	3070 ± 434
Vaupés	3485 ± 314
Vichada	2760 ± 240

TABLE S1 Annual mean ($\overline{x}$) and standard deviation (σ) of rainfall from CHIRPS data during the period 1983–2017 (both included). The information is provided for departments within mainland Colombia (see identical colors in Fig. 1b, note that we have excluded San Andrés and Providencia islands as well as Gorgona and Malpelo Pacific islands). Unit in mm.

	TMI		TMI4		ENSO 1+2		ENSO 3		ENSO 3.4		ENSO 4	
	NS	S	NS	S	NS	S	NS	S	NS	S	NS	S
N_g	7237	2786	13384	10672	9382	3916	10201	6881	10314	7615	9331	7680

TABLE S2 Number of CHIRPS grid cells (N_g) with time lags within the interval [-6, 0) (time lag = 0 not included) for TMI, TMI4 and ENSO oceanic indices: ENSO 1+2, ENSO 3, ENSO 3.4, ENSO 4. Correlations performed cover the period 1983–2017 (both included). NS means that the seasonality has been subtracted by removing the associated monthly climatology at each grid cell, S means that the seasonality is included each month. Note that 1 grid cell has a surface area of $0.05012^\circ \times 0.05012^\circ$.

	TMI4		C		E		CP		EP		Mixed	
	NS	S	NS	S	NS	S	NS	S	NS	S	NS	S
N_g	13384	10672	8985	8167	5966	2157	8190	9641	9774	6753	9968	6646

TABLE S3 Number of CHIRPS grid cells (N_g) with time lags within the interval [-6, 0) (time lag = 0 not included) for TMI4 and Takahashi et al. (2011) (C, P) and Sullivan et al. (2016) (CP, EP, Mixed) oceanic indices. Correlations cover the period 1983–2017 (both included). NS means that the seasonality has been subtracted by removing the associated monthly climatology at each grid cell, S means that the seasonality is included each month. Note that 1 grid cell has a surface area of $0.05012^\circ \times 0.05012^\circ$.

Index	ENSO 1+2	ENSO 3	ENSO 4	ENSO 3.4	C	E	CP	EP	Mixed
TMI4 (1961-2017)	0.739 (-1)	0.762 (-1)	0.509 (-1)	0.681 (-1)	0.457 (-1)	0.651 (-1)	0.199 (21)	0.755 (0)	0.698 (-1)
TMI4* (1981-2017)	0.824 (0)	0.830 (0)	0.548 (-1)	0.735 (-1)	0.485 (-1)	0.727 (0)	0.255 (24)	0.819 (0)	0.761 (0)
TMI5 (1981-2017)	0.813 (0)	0.840 (0)	0.548 (-1)	0.746 (0)	0.487 (-1)	0.714 (0)	0.236 (24)	0.830 (0)	0.769 (0)

TABLE S4 Cross-correlation of original TMI4 and the new TMI4 (renamed as TMI4*) and tMI5, against selected ENSO indices: ENSO 1+2, ENSO 3, ENSO 3.4 and ENSO 4, and other indices more adapted to regionally identify Central Pacific and Eastern Pacific ENSO events such as those of Takahashi et al. (2011) (C, E) and Sullivan et al. (2016) (CP, EP, Mixed), which are described in Section 3.4. Correlations are performed for case studies shown in Fig. S12: TMI4* (4 variables, $z_{20^\circ C}$ instead of Tumaco sea level) and TMI5 (5 variables) and for base period 1986–2015. Note the different time series length shown in parentheses. The highest correlations (in absolute value) and their associated time lag are shown in each panel for all indices. Values provided are significant at 99% (p_{val}<0.01), according to a t-Student two-tailed distribution. Lag times are shown in parenthesis: positive means that TMI4/5 indices lead and negative that TMI4/5 indices follow ENSO indices. At lag = 0 correlated signals are simultaneous, while at other lags time series are shifted several months. Unit of time lag is month.

Index	ENSO$_r$ 1+2	ENSO$_r$ 3	ENSO$_r$ 4	ENSO$_r$ 3.4	C$_r$	E$_r$	CP$_r$	EP$_r$	Mixed$_r$
TMI4$_r$ (1961-2017)	0.204 (0)	0.216 (1)	0.177 (11)	0.196 (-23)	0.174 (11)	0.181 (0)	0.113 (-9)	0.235 (1)	0.197 (1)
TMI4$^*_r$ (1981-2017)	0.206 (2)	0.217 (1)	0.183 (11)	0.178 (-23)	0.183 (11)	0.205 (2)	0.110 (2)	0.234 (1)	0.207 (1)
TMI5$_r$ (1981-2017)	0.203 (0)	0.197 (1)	0.120 (-1)	0.142 (0)	0.118 (-1)	0.182 (0)	0.112 (-27)	0.212 (1)	0.161 (0)

TABLE S5 Same as Table S4 but for the residual components (denoted by the subscript r). The residual components have been computed as explained in Section 3.9.

	TMI4		TMI4*		TMI5	
	NS	S	NS	S	NS	S
N_g	13384	10672	8898	2075	9854	2444

TABLE S6 Number of CHIRPS grid cells (N_g) with time lags within the interval [-6, 0) (time lag = 0 not included) for the original TMI4 (without $z_{20^\circ C}$), TMI4* (which includes $z_{20^\circ C}$ instead of sea level) and TMI5. Correlations cover the period 1983–2017 (both included). NS means that the seasonality has been subtracted by removing the associated monthly climatology at each grid cell, S means that the seasonality is included each month. Note that 1 grid cell has a surface area of $0.05012^\circ \times 0.05012^\circ$.